A Cost-Effective Optoelectronic Cycler for the Durability Testing of Dynamic Windows: Case Studies with Reversible Metal Electrodeposition Devices

| Lorenzo S. Arvisu, Alexis A. | Palma, Shakirul M. | Islam, and Chris | topher J. Barile* |
|------------------------------|--------------------|------------------|-------------------|
|------------------------------|--------------------|------------------|-------------------|

Department of Chemistry, University of Nevada, Reno, NV 89557

*E-mail: cbarile@unr.edu

Abstract

The implementation of dynamic windows that possess electronically tunable transparency is a promising method to increase the energy efficiency of buildings. Long-term dynamic window cyclability is a key issue that has prevented the widespread adoption of many different device architectures. In this manuscript, we have developed an inexpensive (less than \$1,000) optoelectronic cycler to improve dynamic window durability testing. The cycler is programmed to process transmission data to dynamically adjust the voltage profile used for window switching throughout the course of long-term cycling experiments. We demonstrate that this optoelectronic cycler results in significantly improved cycle lives for three different dynamic window chemistries that facilitate reversible metal electrodeposition. Taken together, these results showcase a new tool for the dynamic window research community to improve device cyclability in the laboratory setting.

Keywords

dynamic windows, reversible metal electrodeposition, transparent conductive oxides, cycle life, durability

Introduction

Dynamic windows are devices that change their transparency upon application of a voltage. Due to their ability to control solar radiation, the implementation of dynamic windows increases the energy efficiency of buildings by an average of 10% through lighting, heating, and cooling savings. A wide variety of dynamic window technologies exist including electrochromic materials, polymer-dispersed liquid crystals, and those harnessing reversible metal electrodeposition. Despite the multitude of approaches developed and more than forty years of research, dynamic windows have still not been adopted widely in commercial and residential settings.

One of the major problems hindering the development of dynamic windows is device durability. If these devices are to last the 20-30 years needed for building applications, they must cycle thousands of times without significant degradation. The ASTM-E2141 international standards for dynamic windows stipulate 50,000 cycles with no more than 5% degradation in visible light contrast. Although some companies such as View, Inc. and Halio, Inc. have developed products that pass ASTM-E2141, most dynamic windows produced by academic researchers exhibit inferior durability.

Due to resource constraints, it is generally infeasible to construct durable dynamic windows in the laboratory setting. Achieving long-cycle milestones in an efficient manner requires multichannel testing stations. Even if a window possesses a fast switching time of 1 minute for both tinting and clearing (2 minute cycle time), completing 50,000 consecutive cycles would require nearly 70 days. Furthermore, in a laboratory environment where a standard potentiostat is used to switch dynamic windows, a voltage profile that remains unchanged with cycle number is frequently utilized. However, dynamic glass companies have shown that the best ways to switch dynamic windows without degradation involve complicated voltage profile algorithms.¹¹ These

voltage profiles change through the cycle life of the window to compensate for degradation. For example, the magnitude of voltage might be steadily increased to counteract slowing reaction kinetics. Complex pulsed voltage profiles can also be used.^{12,13}

For all of these reasons, the development and optimization of the complicated voltage profiles needed for durable dynamic windows is a resource-intensive project. To minimize research and development time and costs, in this manuscript, we propose and demonstrate the design of an inexpensive optoelectronically-controlled durability testing apparatus for dynamic windows. The testing apparatus measures the transmission of the dynamic window during cycling and uses that transmission data to intelligently adjust the voltage profile of device switching. By establishing a feedback loop between voltage profile and device optics, an optimal voltage profile throughout the cycle life of the device can be more rapidly developed. Once the ideal voltage profile is determined using this optoelectronic cycler, the voltage profile algorithm could be statically programmed into the power electronics that switch the dynamic window in a commercial product. We demonstrate the operating principles and utility of the designed optoelectronic cycler by testing three different classes of dynamic windows based on reversible metal electrodeposition. Although commercial multichannel battery channels often support the utilization of complex voltage profiles, they do not use optical data to dictate their voltage algorithms as does the system developed here. We anticipate that the adoption of optoelectronic cyclers such as the one described here by other laboratories will greatly accelerate the pace of dynamic window durability research.

Methodology

Optoelectronic Cycler Basics

The optoelectronic cycler switches dynamic windows between their dark and clear states by applying a variable and polarity-reversible direct current (DC) voltage. A light sensor measures

and records the light transmission of the window as it is switching. The sensor data is used to adjust the applied voltages and voltage application times to maintain window performance as the window is cycling between dark and clear states repeatedly.

The test system consists of two Tekpower TP3005P programmable DC power supplies, a Vernier Go Direct Color and Light sensor, a USB-controlled four-channel relay board, and a two-inch stroke linear actuator which are all interfaced via Python on a Windows 10 PC. A block diagram of the dynamic window test system is shown in Figure 1. A video provided in the Supporting Information gives an overview of the optoelectronic cycler components.

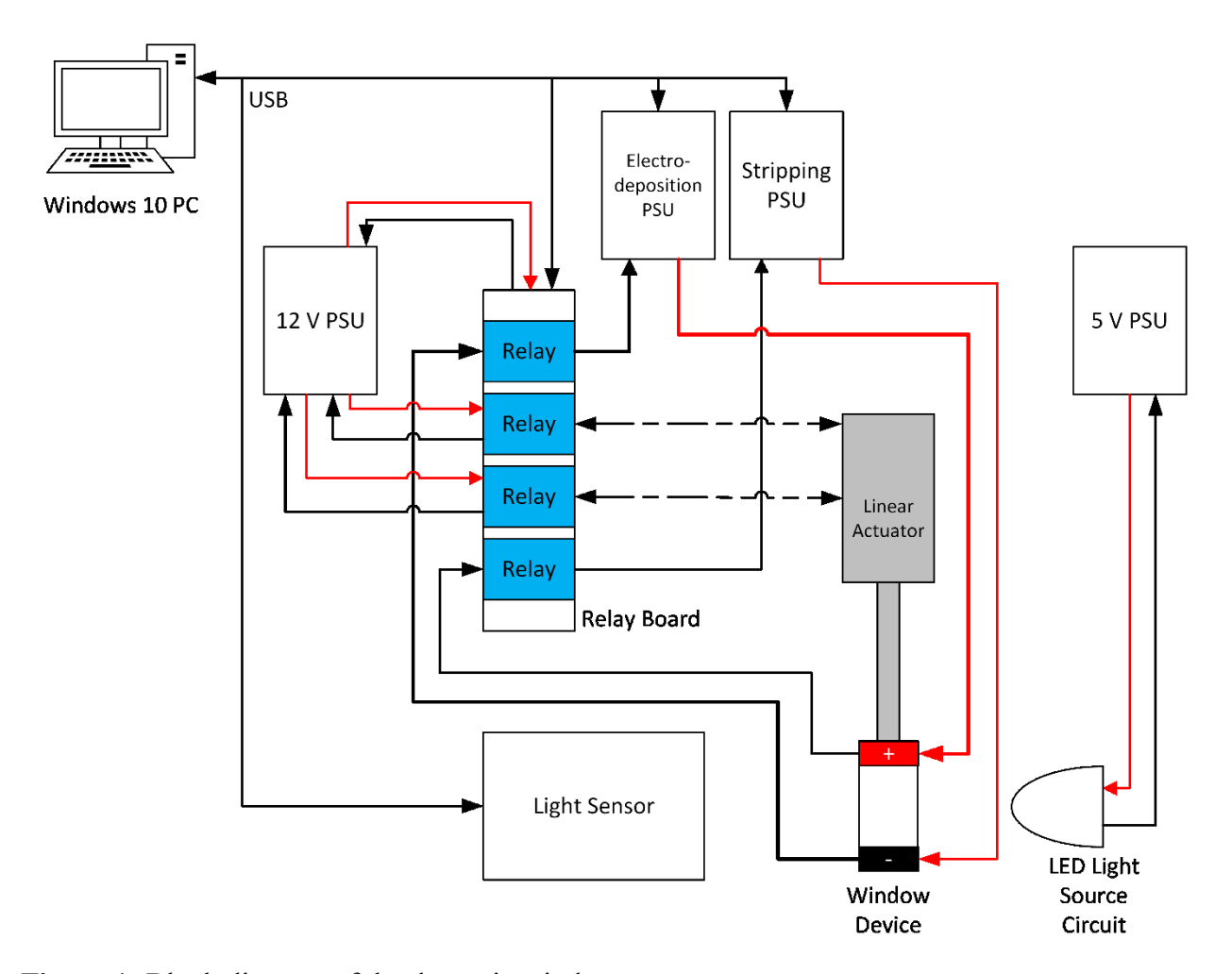


Figure 1: Block diagram of the dynamic window test system.

The two programmable DC power supplies are each switched by an individual single pole double throw (SPDT) relay, which enables the application of voltage in both polarities for the electrodeposition and stripping performed in a window switching cycle. A light sensor measures the light transmitted by a reference light-emitting diode (LED) light source through a window device to measure the window's performance while cycling. A linear actuator switched by two more SPDT relays allows for the window to be moved out of the way of the light sensor path temporarily to perform periodic recalibrations.

The voltage outputs of each power supply are controlled using Python-issued AutoHotKey commands on the accompanying Tekpower EasyPower software that utilizes USB COM port connections to the Windows PC. The relay board and light sensor are also connected via USB, and they are interfaced using Python packages. Light transmission, voltage, and voltage application time are recorded every second and then appended to a comma-separated values (CSV) file after every cycle. Measurements taken at the end of each electrodeposition and stripping period are used to determine if and how the switching parameters need to be adjusted to maintain window performance.

Cost

The bill of materials for the optoelectronic cycler is shown in Table 1. The supplies listed under "Base Supplies" are needed regardless of the number of channels, whereas the "Supplies Needed for Each Channel" are required to add a channel to the system. The total cost of the optoelectronic cycler is \$643.84n + \$254.98, where n is the number of channels. For a single-channel optoelectronic cycler, the estimated cost is therefore \$898.82, a cost that is reasonable for most academic research laboratories.

| Item | Quantity | Price/each | Total |
|------|----------|------------|-------|
| | | | |

| Base Supplies | | | |
|--|----------------------|----------|----------|
| Tekpower TP3005P programmable power supply | 2 | \$119.99 | \$239.98 |
| Breadboard and jumper wires | 1 | \$10 | \$10 |
| Alligator clips | 1 | \$5 | \$5 |
| Subtotal | | | \$254.98 |
| Supplies Needed for Each Channel | | | |
| Tekpower TP3005P programmable power supply | 2 | \$119.99 | \$239.98 |
| 4-channel relay board | 1 | \$22.99 | \$22.99 |
| Vernier GoDirect Color and Light Sensor | 1 | \$93.97 | \$93.97 |
| Generic white LED (3.3 V) | 1 | \$1.00 | \$1.00 |
| 220 ohm resistor | 1 | \$1.00 | \$1.00 |
| 2-inch linear actuator | 1 | \$34.99 | \$34.99 |
| UNR Refurb Windows 10 PC | 1 | \$200.00 | \$200.00 |
| Machine shop materials | 1 | \$50.00 | \$50.00 |
| Subtotal | | | \$643.84 |
| Number of Channels | n | | |
| Total Cost of System | \$643.84n + \$254.98 | | |

 Table 1: Bill of Materials for the Optoelectronic Cycler

Hardware

We now describe in detail the hardware design and development of the dynamic window test system. The test fixture used for the experiments is shown in Figure 2.

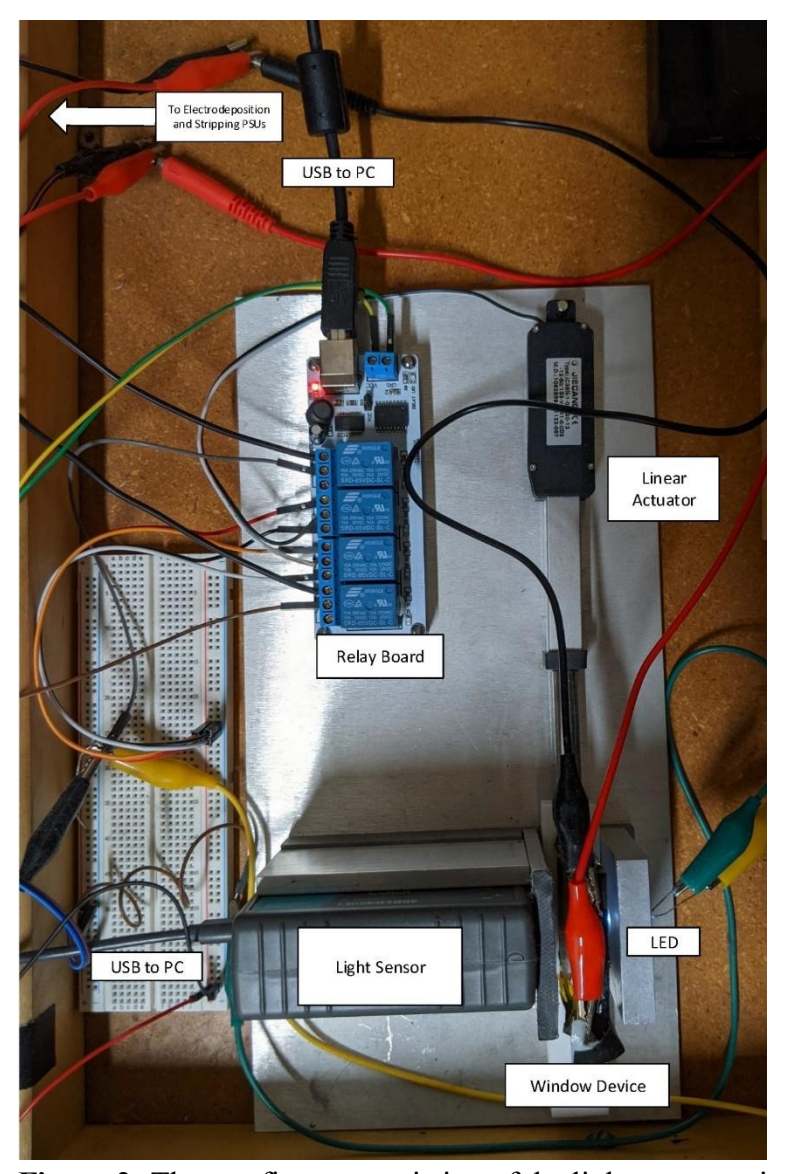


Figure 2: The test fixture consisting of the light sensor, window device, LED circuit, relay board, and linear actuator is shown.

To switch the dynamic windows, an adjustable, reversible polarity voltage is required. Inexpensive programmable power supplies with reversible polarity are not widely available. The dynamic window test system incorporates two programmable 30 V, 5 A Tekpower TP3005P power supplies, which are relatively inexpensive and greatly exceed the power requirements for switching 25 cm² windows, typically 50 mW. ^{14,15} The positive and negative terminals of one power supply are connected to the window device such that it provides the correct polarity for

electrodeposition, and the other is connected in reverse polarity to provide the reverse electrodeposition voltage. To prevent the supplies from shorting between each other, they are each controlled by an electromechanical relay that is normally open. This arrangement also shortens the time to switch between the electrodeposition and stripping states compared to toggling the output states of each power supply.

For accurate measurement of a window's light transmission, a reference light is required. Laser diodes and tungsten-halogen light sources were initially considered, but a simple white LED was selected. The laser diodes only cover a narrow wavelength range and require additional equipment to provide stable output. Our measurements indicate that tungsten-halogen light sources like the Ocean Insight HL-2000 drift less than 0.3% per hour but have limited bulb lifetimes and expensive bulb replacements, especially considering that the test system could be running for weeks at a time. A simple LED with a series resistor to limit current is inexpensive and only exhibited about 1% of drift per hour taking measurements using the system's light sensor for data collection.

To account for LED drift (as well as potential light sensor drift), the optoelectronic cycler incorporates a two-inch linear actuator to move the window device under test out of the path of the light sensor and LED for periodic recalibration. The linear actuator is controlled by the remaining two relays and wired as shown in Figure 2 to enable operating the linear actuator in both directions. The prototype system utilizes two additional TekPower TP3005P power supplies to provide 12 V to the linear actuator and relay board and 5 V to the LED circuit.

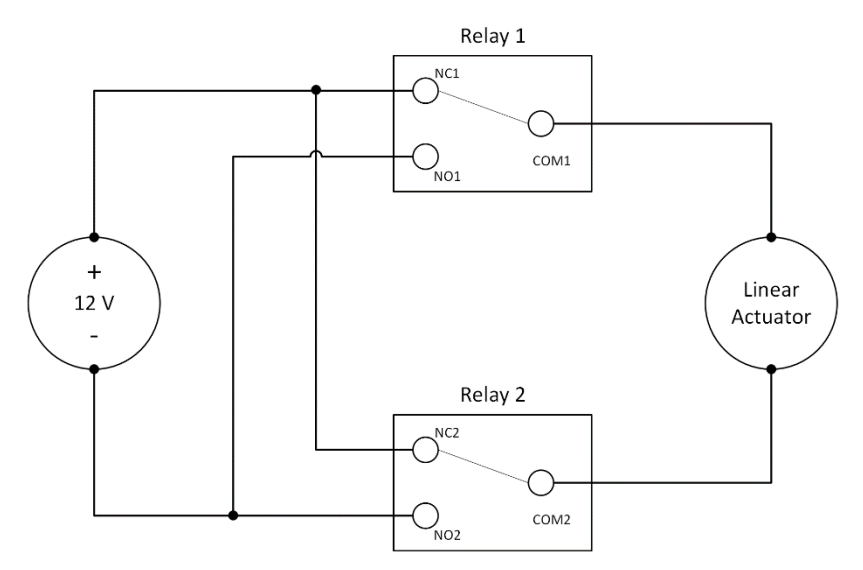


Figure 3: Wiring a motor or linear actuator as shown and activating one relay at a time enables operation in the forward and reverse directions.

The test fixture for the optoelectronic cycler was designed in SolidWorks, and drawings of the parts were sent to the machine shop in the Department of Chemistry at the University of Nevada, Reno to be manufactured. The fixture provides mounting for the light sensor, LED light source, linear actuator, relay board, and test window. The light sensor and LED are aligned with each other and placed as close together as possible to mitigate external light interference, while also leaving room for the linear actuator to move the window sled out of the way for light sensor recalibration. During experiments, the fixture was covered by a box to further minimize external light interference.

Software

The software of the dynamic window test system is written in Python 3 and runs off a Windows 10 PC, which has two copies of the Tekpower EasyPower software installed as well as an installation of AutoHotKey and the Windows Device Console. Python files referred to in this text are provided in whole in the Supporting Information. The two window-switching power supplies, the four-channel relay board, and the light sensor are connected via USB. The module

dynwin.py handles hardware interfacing, system initialization and calibration, window switching operations, and data collection. A separate Python script can use dynwin.py to cycle a window and implement algorithms to monitor light sensor data and adjust voltage and voltage application time as needed. Apart from the cyclic durability testing performed, other tests can be programmed, such as automated shelf-life tests that cycle the window a few times every couple weeks, measuring performance and adjusting parameters as needed.

The two Tekpower TP3005P window-switching power supplies are controlled through their accompanying EasyPower Windows software, which utilizes serial COM port connections over the power supply USB connections. The software collects voltage and current data over time which it stores to a CSV file and displays on a real-time plot. This setup provides an easy way to view power supply status from the PC monitor. To set the voltage of the electrodeposition and stripping power supplies, dynwin.py utilizes the AutoHotKey wrapper ahk to enter the voltage variable values into the appropriate text boxes in the EasyPower software.

The four-channel electromechanical relay board is controlled via a serial COM port connection over USB. The implementation in dynwin.py uses the serial and ftd2xx Python packages to send integer values, which toggle the relays individually. The Vernier Go Direct Color and Light sensor was selected for its variable sample rate, USB connectivity, and the availability of the manufacturer's Python package godirect. The package provides methods to initialize the light sensor and collect light transmission data in lux. The average of five light sensor measurements is collected in a pandas DataFrame every second and at the end of each cycle, appended to a CSV file along with the voltage and voltage application time.

Software Functional Breakdown

The dynamic window test system's Python software consists of the dynwin.py module and a user-generated script incorporating the module. The dynwin.py module contains the base class DynamicWindow that handles interfacing with hardware and other software, system initialization and calibration, window switching, and data collection. The separate user-generated script imports the class and instantiates a DynamicWindow object, using the constructor to set parameters such as initial voltage and voltage application time for the electrodeposition and stripping power supplies, output data filenames, and calibration frequency. The class's methods and variables can then be used to cycle a window device, monitor the light sensor data, and adjust switching parameters as necessary.

PrusBlueTest.py

As an example, a flowchart of the script PrusBlueTest.py used to test the Bi-Prussian blue window chemistry is shown in Figure 4 to break down the dynamic window test system functionality and the algorithm implemented to improve cycle life. The algorithm parameters are shown in Table 2, and some parameters are passed as arguments to the DynamicWindow constructor. The window device under test is cycled in an infinite while loop. There is a warmup period of 200 cycles (warmupCycles = 200) in which no changes are made to the initial switching parameters. The minimum and maximum light transmission measurements from the subsequent twenty cycles are averaged to generate target transmission values for the algorithm. After the target values are obtained, five-cycle averages (averagingFreq = 5) of the minimum and maximum light transmission measurements are individually compared to their target values:

$$\frac{darkAvg - darkTarget}{darkTarget} > threshDark$$

$$\frac{clearAvg-clearTarget}{clearTarget} < -threshClear$$

If a comparison is true, then the voltage for that mode is increased by the voltage step value. A default value of 0.01 V is used for both electrodeposition (vStepDark = 0.01 V) and stripping (vStepClear = 0.01 V). Another five cycles are run and averaged, and the averages are compared to the target values again. If performance remains within the threshold values, then the cycling continues until performance falls out of range again. If the performance does not improve, the voltage is increased by the voltage step value again and another five cycles are run to evaluate the effect. This process will continue until performance improves, or the maximum voltage is reached. At this point, the voltage application time can be increased by the time step value (tStepDark or tStepClear) in the same manner as the voltage until the maximum switching time is met.

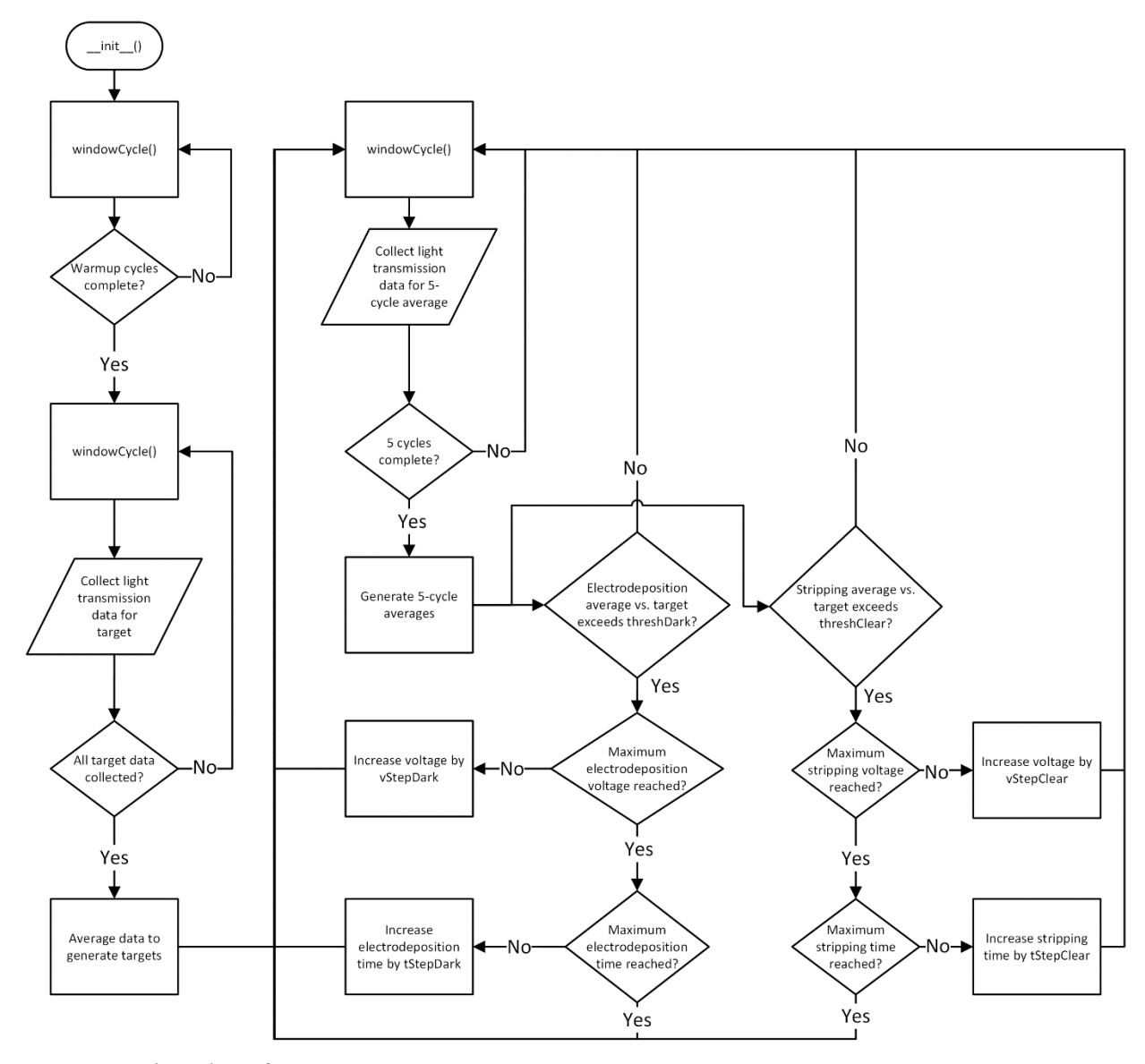


Figure 4: Flowchart for PrusBlueTest.py

| Parameter | Bi-Cu Algorithm 1 | Bi-Cu Algorithm 2 | Bi-Cu Algorithm 3 | Zn | Prussian Blue |
|--------------|----------------------|----------------------|----------------------|--------|------------------|
| warmupCycles | 50 | 50 | 50 | 0 | 200 |
| voltageDark | -0.5 V | -0.5 V | -0.5 V | -0.5 V | -0.6 V |
| vMaxDark | -0.6 V | -0.6 V | -0.6 V | -1 V | -2 V |
| vStepDark | 0.01 V | 0.01 V | 0.01 V | 0.01 V | 0.01 V |
| timeDark | 60 s | 60 s | 60 s | 60 s | 20 s |

| tMaxDark | 300 s |
|---------------|--------|--------|--------|--------|--------|
| tStepDark | 1 s | 1 s | 5 s | 1 s | 1 s |
| threshDark | 1% | 0.25% | 0.25% | 5% | 10% |
| voltageClear | 0.7 V | 0.7 V | 0.8 V | 0.8 V | 1.4 V |
| vMaxClear | 0.8 V | 0.8 V | 0.8 V | 1.2 V | 1.4 V |
| vStepClear | 0.01 V |
| timeClear | 120 s | 120 s | 120 s | 120 s | 45 s |
| tMaxClear | 300 s |
| tStepClear | 1 s | 5 s | 5 s | 1 s | 5 s |
| threshClear | 1% | 1% | 1% | 5% | 5% |
| averagingFreq | 20 | 20 | 20 | 1 | 5 |
| calCycleFreq | 2 | 2 | 2 | 2 | 2 |

Table 2: Algorithm parameters

dynwin.py

When a DynamicWindow object is created, the constructor function __init__() runs once to assign variables from the constructor parameters and initialize the system. The coordinate locations of EasyPower UI elements used by AutoHotKey are stored here. The relay board must be set up with bit bang mode using the ftd2xx package before a serial connection is made. The light sensor is initialized, and multithreading is set up for continuous light sensor data collection while cycling windows. Data and backup folder directories are created if they do not exist, and the data file is created with the name set by the constructor parameter datafile along with the time and date. The constructor function then prompts the user from the terminal to place the window in the test fixture then hit <Enter> to perform initial light sensor calibration. Once initialization is complete, the user is prompted once more to hit <Enter> to begin the usergenerated script. A flowchart of the constructor function __init__() is shown in Figure 5.

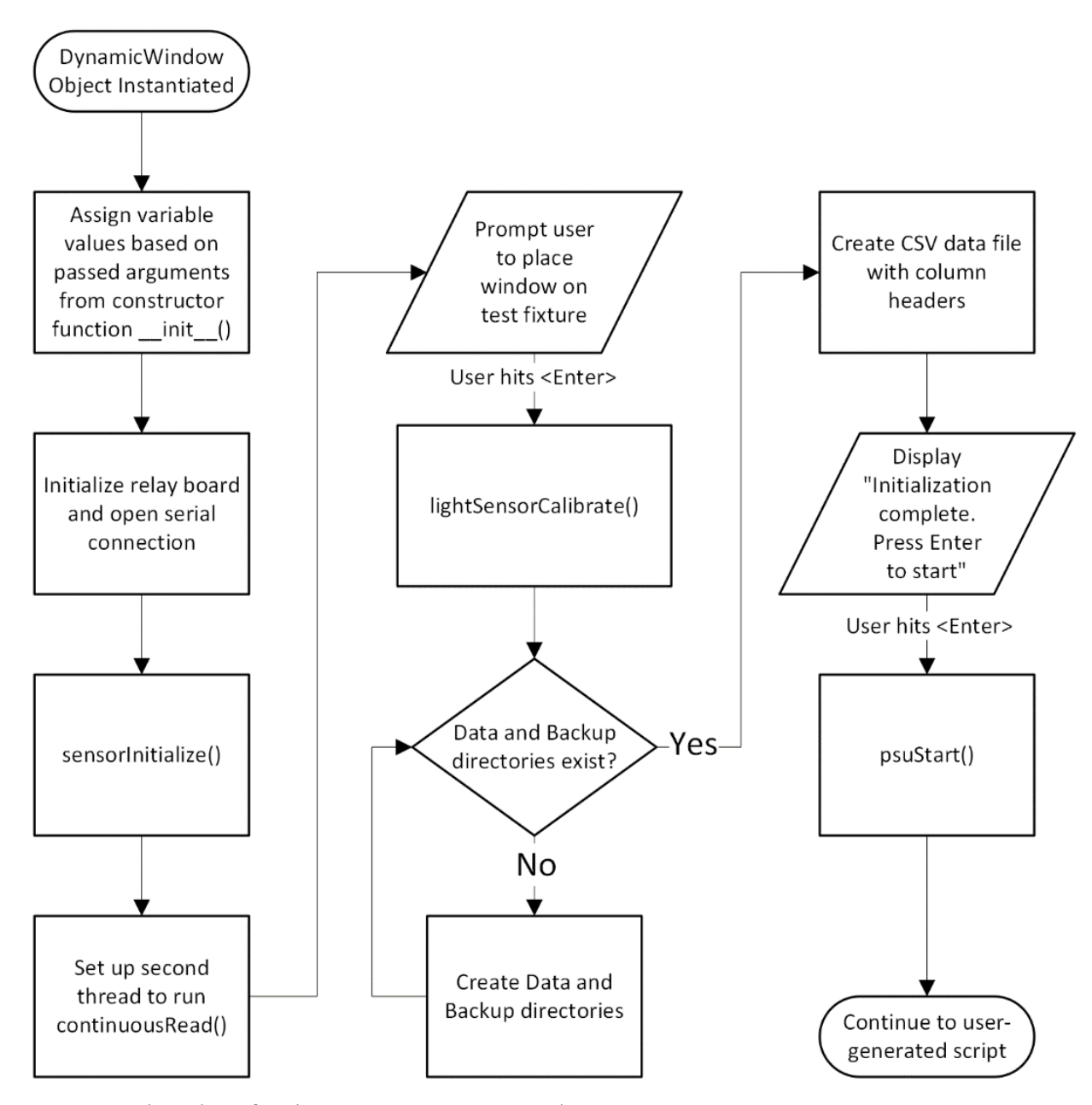


Figure 5: Flowchart for the DynamicWindow class constructor __init__()

The function sensorInitialize() uses methods from the godirect package to connect to the Vernier Go Direct Light and Color sensor and set it up for data collection from the visible light sensor. If initialization fails, the function will attempt to restart the device from software using sensorRestart() and then try sensor initialization again. If initialization still

fails, the function will output a message prompting the user to try physically restarting the light sensor device while attempting to restart and initialize from software every 60 s.

The function lightSensorCalibrate() operates the relays corresponding to the linear actuator to move the window device under test out of the path of the light sensor and LED light source using linActuator(). A light sensor measurement is taken and stored using sensorRead(), and the linear actuator is reversed to return the window device to its original position.

The function sensorRestart() uses the Windows Device Console (devcon.exe) to disable and enable the Vernier Go Direct Light and Color sensor device. If the light sensor is not functioning correctly after days of data collection, the dynamic window test system will try restarting the device from software to continue the program with minimal interruption or data loss before pausing the program and prompting the user to physically restart or replace the sensor.

The function sensorRead() sets the light sensor to run at a frequency defined in the constructor function, collects light transmission data in lux for 1 s, and returns the average of the measurements. The dynamic window test system's default sampling rate is set to 5 Hz. Despite the sensor being capable of a 1000 Hz sample rate, the godirect package is not able to return data at rates above 5 Hz. If the light sensor takes more than 1 s or fails to return data, the function will attempt to restart the light sensor every 10 s using sensorRestart() and sensorInitialize().

The function transmission() uses the calibration variable calVal and the data returned from sensorRead() to calculate the percentage of light transmitted through the window device compared to open air:

$$light\ transmission\ (\%) = \frac{measurement\ (lux)}{calibration\ measurement\ (lux)} \times 100\%$$

The relay board functions relayDark(), relayClear(), linActuator(), and relaysOff() send integer values in binary over the serial connection to enable or disable individual relays. The functions for the relays controlling the electrodeposition and stripping power supply outputs, relayDark() and relayClear(), take a Boolean (True or False) argument to determine whether to enable their respective relays or to call relaysOff(). The linActuator() function accepts the arguments 1 and -1, which determine the direction of operation for the linear actuator. When the argument is 1, the corresponding relay switches on for 3 s and allows the linear actuator to retract. When the argument is -1, the other relay switches on for 4 s and allows the linear actuator to extend to its limit, ensuring that the window device is returned to its original position. The function relaysOff() sends 0 to the relay board, ensuring that all relays are off.

The function psuStart() initializes the electrodeposition and stripping power supplies with their current limits and initial voltages using the AutoHotKey wrapper ahk. This process is accomplished using the coordinates for the EasyPower user interface (UI) elements stored in the constructor function to have AutoHotKey click on the appropriate text boxes and type the according values in. The EasyPower windows for each power supply must be "snapped" manually to opposite sides of the monitor to ensure that the coordinate locations of the text boxes do not change, shown in Figure 6. If the Windows PC is to be run on a different monitor resolution, the coordinate locations would change, but these values can easily be re-recorded.



Figure 6: The Tekpower EasyPower windows for the electrodeposition and stripping power supplies must be "snapped" to the same position to ensure that the coordinates of the UI elements remain the same.

The function windowSwitch() handles the actions for half a cycle, either electrodeposition or stripping, depending on what the arguments for relay, text, voltage, enter, and seconds correspond to. The voltage of the power supply is set using ahk and the text, voltage, and enter parameters. The continuousReadPermission flag used for multithreading is set before the relay is turned on, enabling the thread running continuousRead() to collect data while the window is switching. Multithreading ensures that the voltage is applied to the window device under test for the specified amount of time if data collection takes longer or shorter than expected. If light sensor data collection takes longer than

expected, the windowSwitch() function will wait until the continuousReadPermission flag is cleared, which indicates that data collection is complete.

The function continuousRead() runs in a separate thread. Inside an infinite loop, the function waits for the continuousReadPermission flag to be set, and depending on if the system is in electrodeposition (clearingStatus = False) or stripping mode (clearingStatus = True), collects transmission() data for the appropriate amount of time and appends the data to the corresponding pandas DataFrame using dataFrameAppend(). When data collection is complete, the continuousReadPermission flag is cleared, signaling the main thread to continue.

The function dataFrameAppend() takes a single measurement as an argument and appends it to the DataFrame dataToWrite, with formatting dependent on if the system is in electrodeposition (clearingStatus = False) or stripping mode (clearingStatus = True).

The function windowCycle() performs one full cycle on the window device under test. The function first checks the cycleCount, and if it is divisible by calCycleFreq (default value of 2), calls lightSensorCalibrate() to recalibrate the light sensor. The clearingStatus flag is first set to False, and windowSwitch() is called with the arguments relayDark(), textDarkV, voltageDark, enterDarkV, and timeDark to perform electrodeposition. A final transmission() measurement is appended to the DataFrame dataToWrite and numpy array sensorDataDark. The array can be accessed from the user-generated script to monitor window performance. The clearingStatus flag is then set to True, and the windowSwitch() and additional transmission() recording is repeated with functions and variables corresponding to the stripping mode. If the system is

configured for periodic extended stripping times as in *Bi-Cu Algorithm 3*, the function will check if cycleCount is divisible by longStripCycleFreq and change the stripping time from timeClear to tLongStrip for the cycle. When the cycle is complete, the data is written to the CSV file using writeData(), the DataFrame dataToWrite is cleared, and cycleCount is incremented by 1.

The function writeData() calls writeCsv() and handles pausing the test if the data file cannot be accessed for reasons like the file being open elsewhere. A backup is also created by copying the data file to the backups folder. The function writeCsv() uses the csv package to open the data file and append the data from dataToWrite.

Dynamic Window Construction

Chemicals were obtained from commercial sources and used as received without further purification. Tin-doped indium oxide (ITO) on glass electrodes (Xin Yan, Inc., $10 \Omega \text{ sq}^{-1}$) were first cleaned by sonicating in H₂O with 5% Extran solution for 5 min. The substrates were next washed successively with water and isopropanol before they were sonicated in isopropanol for 5 min. Finally, the ITO samples were dried under a stream of air.

For windows tested with Bi electrolytes (Bi-Cu windows or Bi-Prussian blue windows), the cleaned ITO on glass electrodes were modified with Pt nanoparticles. To form a layer of Pt nanoparticles, the electrodes were first immersed in a 10 mM solution of 3-mercaptopropionic acid in ethanol for 24 hours. The electrodes were rinsed with ethanol and water before immersing them in a dispersion of Pt nanoparticles in water (3 nm diameter, 250 ppm, Sigma-Aldrich) for an additional 24 hours. Lastly, the electrodes were washed with water and heated for 20 min at 275°C under air.

All dynamic windows were two-electrode devices with an area of 25 cm². Bi-Cu windows were assembled according to previous literature procedures.¹⁶ Cu tape was applied along the four edges of the working electrode to make uniform electrical connection to the ITO on glass. The counter electrode consisted of a Cu foil frame placed on top of a nonconductive glass sheet. To seal the device, butyl rubber was applied around the perimeter of the two electrodes. After device sealing, an aqueous-based Bi-Cu gel electrolyte was injected through the sealant via syringe. The electrolyte was comprised of 5 mM BiCl₃, 15 mM CuCl₂, 10 mM HCl, and 1 M LiBr with 3.0 wt. % hydroxyethylcellulose.

Zn windows were constructed in an analogous manner to the Bi-Cu windows as reported previously.¹⁷ A Zn foil frame was used, and the electrolyte consisted of 500 mM Zn(CH₃COO)₂, 900 mM KCl, and 2.0 wt. % hydroxyethylcellulose.

Bi-Prussian blue windows were built according to a previous literature procedure.¹⁵ These windows contain a Bi-coated Pt-modified ITO on glass working electrode and a Prussian blue counter electrode. In this manner, the windows are constructed in their dark state.

To create the counter electrode, Prussian blue thin films were first deposited electrochemically on ITO on glass surfaces in a three-electrode cell with ITO on glass as the working electrode, Ag/AgCl/3 M KCl (Edaq, Inc.) as the reference electrode, and a Pt wire as the counter electrode. The perimeters of the ITO substrates were covered with conductive Cu tape. This Cu tape was then covered with non-conductive Kapton tape to ensure no Cu ions leached into the Prussian blue electrodeposition electrolyte. Prussian blue was electrodeposited on the ITO electrode by using chronoamperometry at +0.5 V for 6 min in an aqueous electrolyte of 5 mM FeCl₃, 5 mM K₃Fe(CN)₆, and 200 mM KCl. After electrodeposition, the ITO electrodes were rinsed gently with water and allowed to dry in air at room temperature.

To electrodeposit Bi on the Pt-modified ITO substrates prior to device stack assembly, a three-electrode cell was used with Pt-modified ITO on glass as the working electrode, Ag/AgCl/3 M KCl (Edaq, Inc.) as the reference electrode, and a Pt wire as the counter electrode. The edges of the ITO electrodes were covered with Cu tape followed by non-conductive Kapton tape. An aqueous electrolyte consisting of 5 mM BiCl₃, 1 M KBr, and 10 mM HCl was used during Bi electrodeposition. A voltage of -0.6 V was held for 60 s in this electrolyte to elicit Bi electrodeposition.

Working ITO electrodes modified with Bi and Pt and counter ITO electrodes modified with Prussian blue were assembled together to form the Prussian blue dynamic windows using butyl rubber as the sealant with an interelectrode spacing of 4 mm. A Bi gel electrolyte was formed by adding 3.0 wt. % hydroxyethylcellulose to an aqueous liquid electrolyte containing 15 mM BiCl₃, 3 M KBr, and 10 mM HCl.

Results and Discussion

To test the efficacy of the designed optoelectronic cycler, we evaluated the durability of dynamic windows that function via reversible metal electrodeposition of metals (RME) under different cycling algorithms. In particular, we constructed three different classes of dynamic windows based on different metal electrodeposition chemistries (Bi-Cu, Zn, and Bi-Prussian blue). Before describing the various performances of these devices, we first introduce the operating principles of dynamic windows based on RME.

RME windows become dark when a voltage is applied to elicit a reduction reaction causing metal deposition on a transparent conducting working electrode from an electrolyte containing colorless metal ions.¹⁸ To balance the charge passed during deposition, a counter electrode facilitates an oxidation reaction. Depending upon the device architecture, this counter reaction can

be either the oxidation of a metal frame to metal ions or an intercalation-based oxidation on a plane-parallel transparent conductor. 19,20

We first tested the optoelectronic cycler with Bi-Cu RME windows. These windows consist of a Pt-modified ITO working electrode and a Cu frame counter electrode (Figure 7A). Transparent Pt nanoparticles (3 nm in diameter) serve as a seed layer to enhance metal deposition uniformity and kinetics as has been described previously. The Bi-Cu electrolyte supports the coelectrodeposition of Bi and Cu, which gives rise to a uniform color-neutral electrodeposit with good electrochemical reversibility. 16

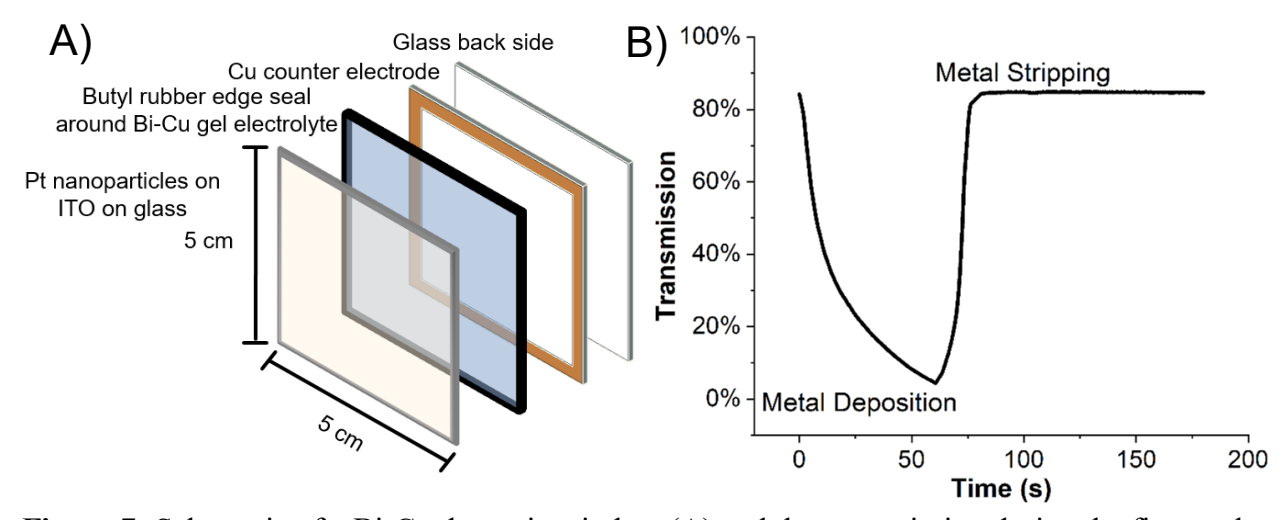


Figure 7: Schematic of a Bi-Cu dynamic window (A) and the transmission during the first cycle of the device (B). Metal deposition was elicited by holding the device at -0.5 V for 60 s followed by metal stripping at +0.7 V for 120 s.

Figure 7B displays the white LED transmission profile of a Bi-Cu dynamic window during its first switching cycle. The spectrum of the white LED emission is shown in Figure S1. The window is first polarized at -0.5 V for 60 s to induce metal electrodeposition on the ITO working electrode, which causes its transmission to decrease from 85% to a minimum value of 4%. The contrast ratio, defined as the difference between the maximum and minimum transmission values during a switching cycle, of this window is therefore 81%. After window tinting, the voltage of

the device is switched to +0.7 V for 120 s, which causes the deposited metal to dissolve back into the electrolyte. As a result, the transmission of the window returns to its original value.

The window was further switched for 203 consecutive cycles. Figure 8A displays the normalized contrast ratio of the Bi-Cu window during cycling. The contrast ratios here are normalized to the maximum contrast ratio achieved during cycling. Therefore, the observation that the normalized contrast ratio reaches a value of 60% after 203 cycles means that the contrast ratio degraded by 40% over the course of 203 cycles. In other words, the absolute contrast ratio decreased to about 49% (60% * 81%) after the 203 cycles. For all cycling data presented in this manuscript, we use a cycling cutoff of 60% for the normalized contrast ratio so that we can make uniform comparisons across the various window chemistries and voltage algorithms utilized. The standard deviation error bars for the cycle lives of RME dynamic windows determined in this manner range from 10-15%. Fluctuations in cycle lives across devices are due to numerous irreproducible factors including variations in the initial surface morphology of the commercially used ITO across substrates and slight differences in device geometry that result from constructing the devices by hand in a laboratory environment.

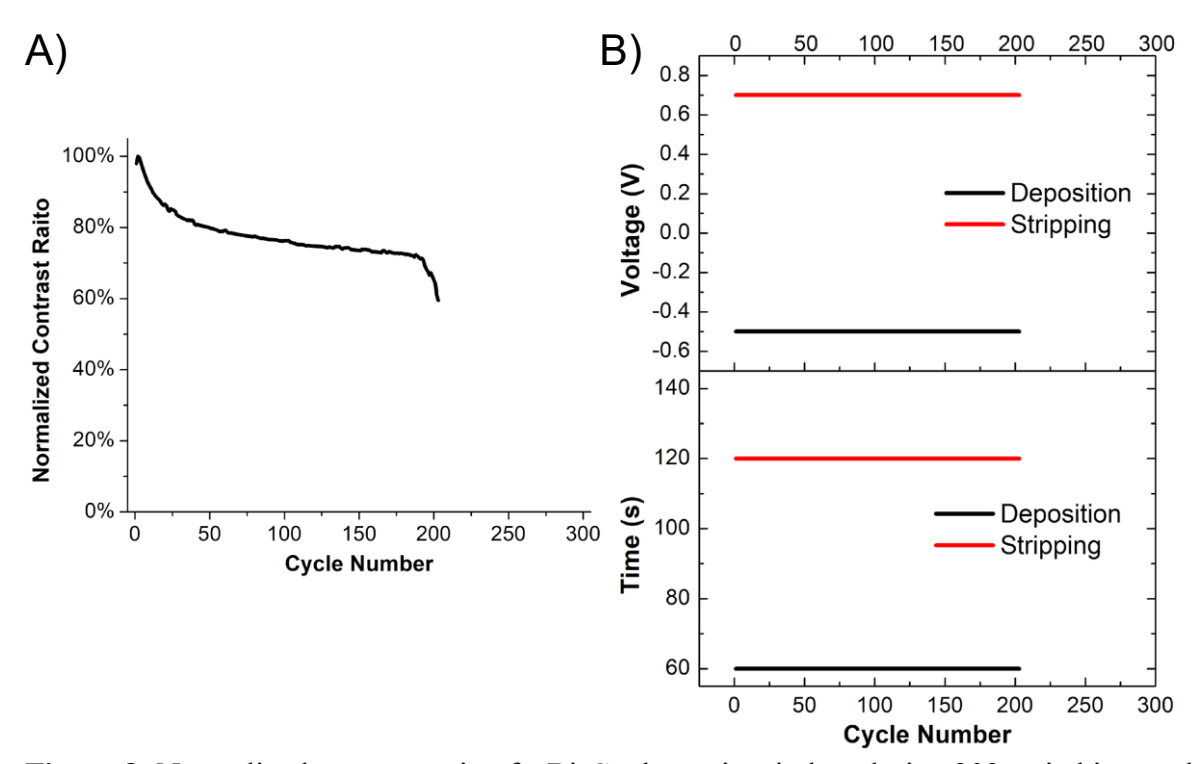


Figure 8: Normalized contrast ratio of a Bi-Cu dynamic window during 203 switching cycles (A) and the constant voltage (B, top panel) and time (B, bottom panel) profiles used for both deposition (black line) and stripping (red line) during cycling.

The absolute maximum and minimum transmission values of the Bi-Cu window during the 203 cycles are displayed in Figure S2. These data provide information about how the window degrades during cycling. In particular, while the maximum transmission (black line) stays relatively constant over the first 180 cycles, the minimum attained transmission (red line) progressively increases during the same period of time. These results indicate that the metal electrodeposition process becomes less effective at blocking light throughout the first 180 cycles. In contrast, during the last 23 cycles, the maximum transmission (black line) decreases significantly, indicating that a decrease in the speed of metal stripping further degrades the normalized contrast ratio of the device.

The top panel in Figure 8B shows that during these 203 cycles, the voltages used for window tinting and clearing were held constant at -0.5 V and +0.7 V, respectively. Similarly, the

bottom panel in Figure 8B shows that the times used for window tinting and clearing were held constant at 60 s and 120 s, respectively, during cycling. In this manner, this experiment serves as a control to compare against windows using voltage and time parameters that vary during cycling based on algorithms controlled by the optoelectronic cycler.

Bi-Cu Algorithm 1

Because both the maximum and minimum transmission values degrade during cycling in the constant voltage and constant time experiment, we utilized an optoelectronic algorithm that progressively increases the magnitude of the deposition and stripping voltages during cycling in an attempt to increase device cycle life. The details of how the algorithm works are provided in the methodology section of this manuscript, and the cycling results are presented in Figures 9 and S3. The data show that with the algorithm the Bi-Cu dynamic window switches 274 times before reaching the 60% normalized contrast ratio cutoff value. By comparison, without the algorithm the window switches only 203 cycles before reaching the same normalized contrast ratio (Figure 8).

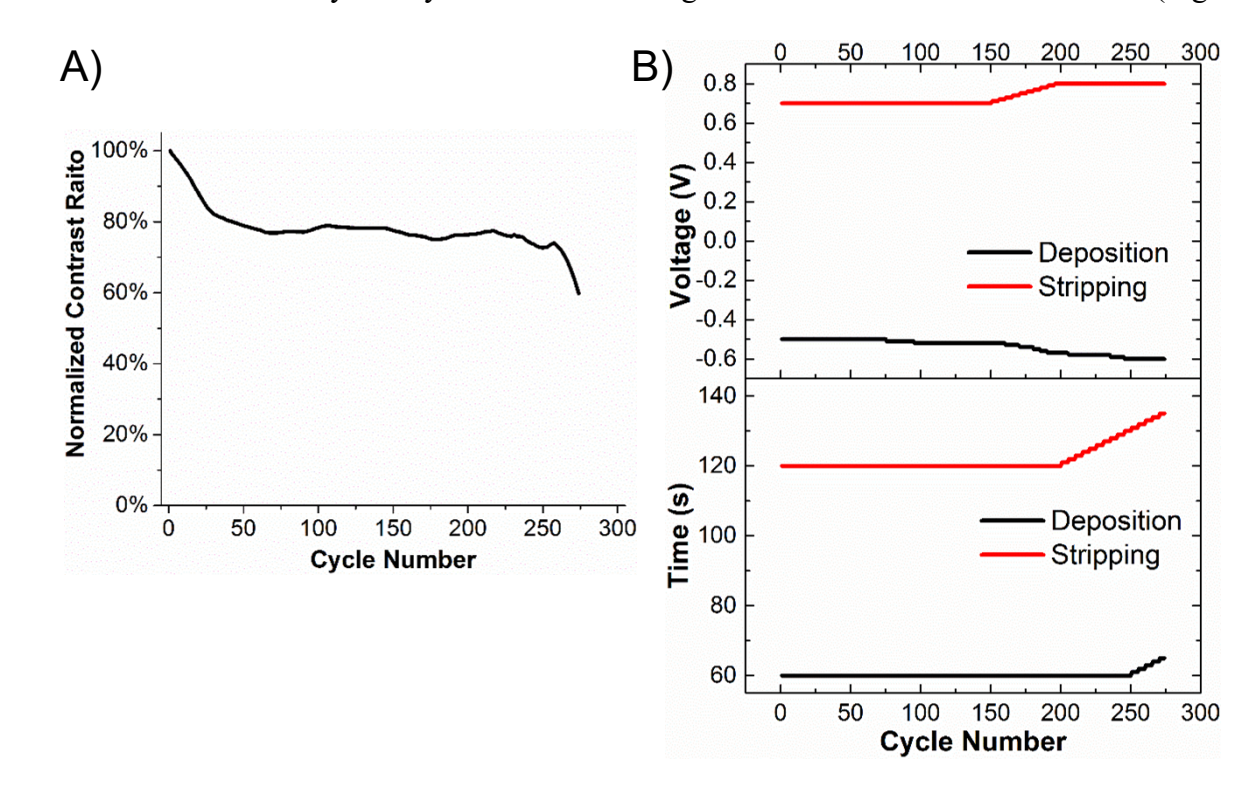


Figure 9: Normalized contrast ratio of a Bi-Cu dynamic window during 274 switching cycles (A) and the voltage (B, top panel) and time (B, bottom panel) profiles used for both deposition (black line) and stripping (red line) during cycling.

During cycling of the device using the algorithm, the deposition voltage becomes progressively more negative from -0.5 V to -0.6 V (Figure 9B, top panel, black line). The higher driving force of the applied voltage allows the window to maintain a steady optical contrast, while the control experiment at constant voltage shows that the degradation in contrast ratio would otherwise occur. Once a deposition voltage of -0.6 V is reached, the algorithm no longer changes the voltage because previous studies indicate that at voltages more negative than -0.6 V, H₂ evolution, a gaseous side product that must be avoided during device operation, occurs on the ITO working electrode.²² Instead, the algorithm progressively increases the -0.6 V deposition time (Figure 9B, bottom panel, black line). The increase in deposition time, however, only occurs after 250 cycles. In other words, the algorithm enables the cycle life of the window to increase from 203 cycles to 250 cycles without slowing down the darkening speed of the device.

The algorithm also adjusts the stripping voltage and time during cycling in an attempt to keep the contrast ratio steady during cycling. As such, the stripping voltage becomes progressively more positive from 0.7 V to 0.8 V while the window switches (Figure 9B, top panel, red line). Because voltages greater than 0.8 V degrade ITO, the algorithm does not increase the voltage beyond 0.8 V and instead increases the stripping time (Figure 9B, bottom panel, red line).

Together, these adjustments made by the algorithm give rise to the normalized contrast ratio profile shown in Figure 9A. We note that for the Bi-Cu chemistry, the algorithm implements an initial 50 cycle "warm-up" period before it begins adjusting the voltage parameters. For this reason, the normalized contrast ratio steadily decreases during the initial 50 cycles. From cycles 50 to 255, however, the normalized contrast ratio is relatively stable as the algorithm dynamically

adjusts switching parameters. Beyond cycle 255, the normalized contrast ratio rapidly declines to the 60% cutoff value. The maximum and minimum transmission values measured during each cycle are shown in Figure S3. The data reveal that after cycle 255, it is the maximum transmission value that declines rapidly, which is the origin of the rapidly declining contrast ratio. This result indicates that beyond cycle 255, the algorithm was not able to change the stripping time fast enough to maintain a steady normalized contrast ratio during cycling.

Bi-Cu Algorithm 2

In an attempt to increase the cycle life of the window, we cycled a Bi-Cu dynamic window with an adjusted algorithm. This new algorithm increases both the stripping and deposition times more rapidly with 5 s increments instead of 1 s increments (tStepClear = tStepDark = 5 s). The modified algorithm also utilizes more sensitive threshold arguments (threshClear = threshDark = 0.25%). Both of these modifications make *Bi-Cu Algorithm 2* switch its voltage and time parameters faster than *Bi-Cu Algorithm 1*.

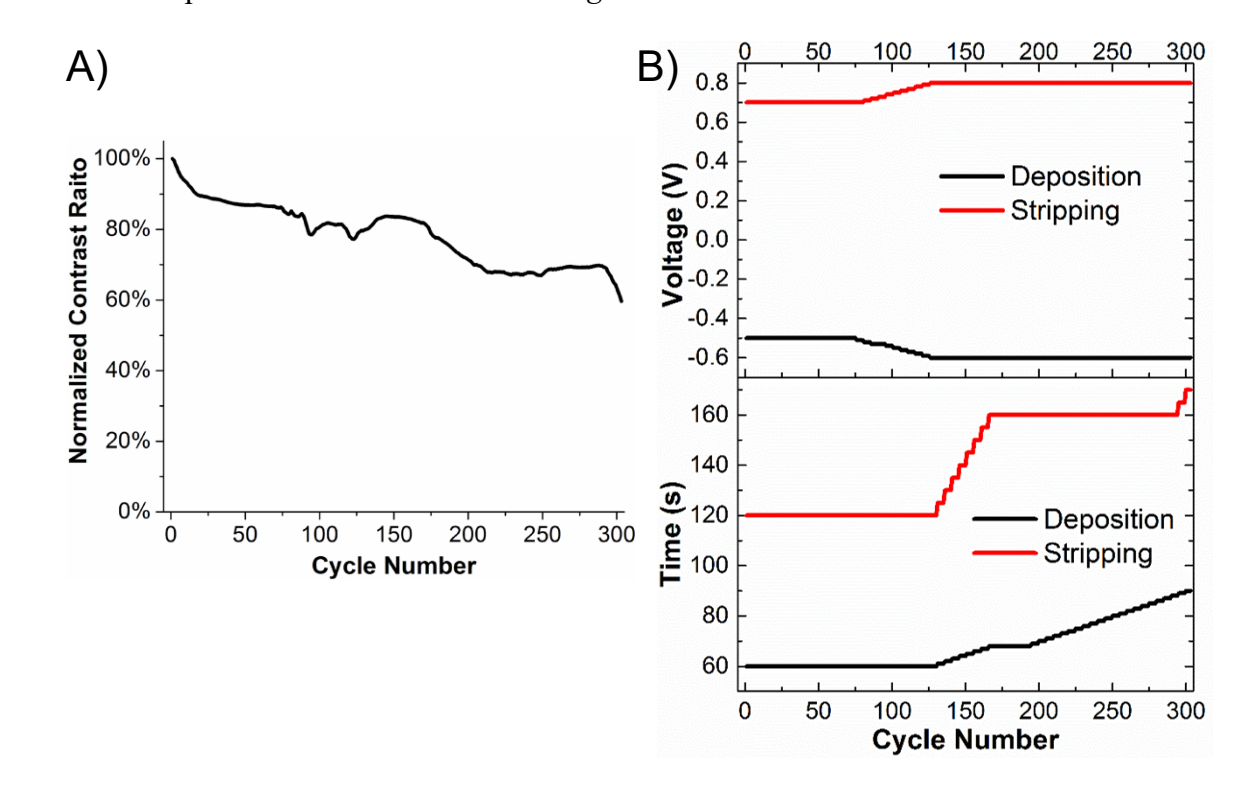


Figure 10: Normalized contrast ratio of a Bi-Cu dynamic window during 303 switching cycles (A) and the voltage (B, top panel) and time (B, bottom panel) profiles used for both deposition (black line) and stripping (red line) during cycling.

Figures 10 and S4 display the results of switching a dynamic window using *Bi-Cu Algorithm 2*. This device cycles 303 times before reaching the 60% normalized contrast ratio cutoff value (Figure 10A), which is a significant improvement over the 274 cycles achieved using *Bi-Cu Algorithm 1*. This increased cycle life is a direct result of the increased sensitivity of the modified algorithm. However, the increased sensitivity of the algorithm causes the deposition and stripping speeds to decrease after around only 130 cycles. This accelerated onset of increased deposition and stripping times occurs as a result of the cutoff voltages being reached earlier.

Taken together, these results demonstrate that there is an important balance to achieve in developing optoelectronic switching algorithms. If the adjustability of the switching parameters in the algorithm is not sensitive enough, the cycle life of a window will be poor. On the other hand, if the adjustability of the switching parameters is too sensitive, the cycle life will be improved, but at the cost of slower switching speeds.

Bi-Cu Algorithm 3

In both *Bi-Cu Algorithms 1* and 2, a rapid decline in the maximum transmission value at the end of cycling resulted in the normalized contrast ratio degrading to the 60% cutoff value. These findings suggest that appropriate changes of the stripping portion of the algorithm could further increase cycle life. More broadly, metal stripping in dynamic windows based on reversible metal electrodeposition is a reoccurring issue during long-term cycling.^{19,23} One of the most common reported cycling issues is that metal electrodeposits accumulate in grain boundaries of ITO and are not able to dissolve back into the electrolyte during a typical stripping cycle. If these

deposits are simply slow to strip, a longer stripping time should prevent the accumulation of these deposits and increase device cycle life.

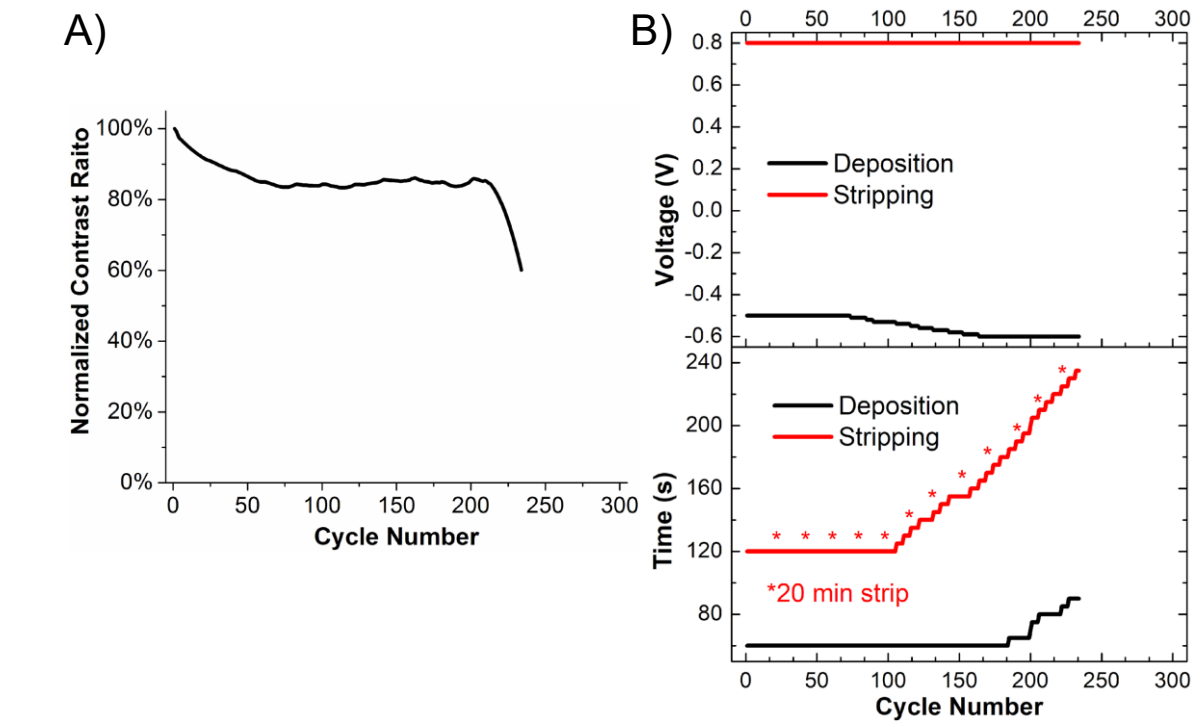


Figure 11: Normalized contrast ratio of a Bi-Cu dynamic window during 234 switching cycles (A) and the voltage (B, top panel) and time (B, bottom panel) profiles used for both deposition (black line) and stripping (red line) during cycling. The red asterisks indicate that a 20 minute stripping time was used during that cycle instead of the plotted time.

To test this hypothesis, we designed an algorithm that dramatically increased both the driving force and time for metal stripping. In this *Bi-Cu Algorithm 3*, we implemented a constant stripping voltage of at the 0.8 V maximum value (Figure 11B, top panel, red line). Furthermore, every 20 cycles, we programmed the algorithm to strip at 0.8 V for 20 minutes (Figure 11B, bottom panel, red asterisks), instead of the typical 120 s, in an attempt to dissolve any electrodeposits accumulated in ITO grain boundaries.

The normalized contrast ratio data in Figure 11A (and derived from data in Figure S5) indicate that the Bi-Cu dynamic window with this aggressive stripping profile reaches the 60% cutoff value in only 234 cycles as compared to the 303 cycles achieve with *Bi-Cu Algorithm 2*.

These findings demonstrate that increasing the driving force or time for stripping does not result in enhanced device cycling. From a chemical perspective, these results indicate that it is not simply slow stripping kinetics of residual metal electrodeposits that limits device cycle life. More importantly, however, the results illustrate how optoelectronic algorithms can be used to test chemical hypotheses with respect to dynamic window durability.

Zn Windows

Having studied the effect of various algorithm parameters on the cycling of Bi-Cu dynamic windows, we next used the optoelectronic cycler to switch devices based on the reversible electrodeposition of Zn. The architecture of Zn dynamic windows is the same as Bi-Cu devices except that the electrolyte contains Zn salts and the counter electrode is Zn. Due to the high concentration of Zn electrolytes, Zn dynamic windows have the advantage of being able to switch to a very dark state (less than 0.1 %) within 60 s (Figure S6). The downside of Zn chemistry is the poor cyclability of Zn windows. In particular, stripping speeds progressively decrease during cycling. This issue is attributed to the accumulation of insulating ZnO and Zn(OH)₂ deposits during each window tinting cycle.²⁴

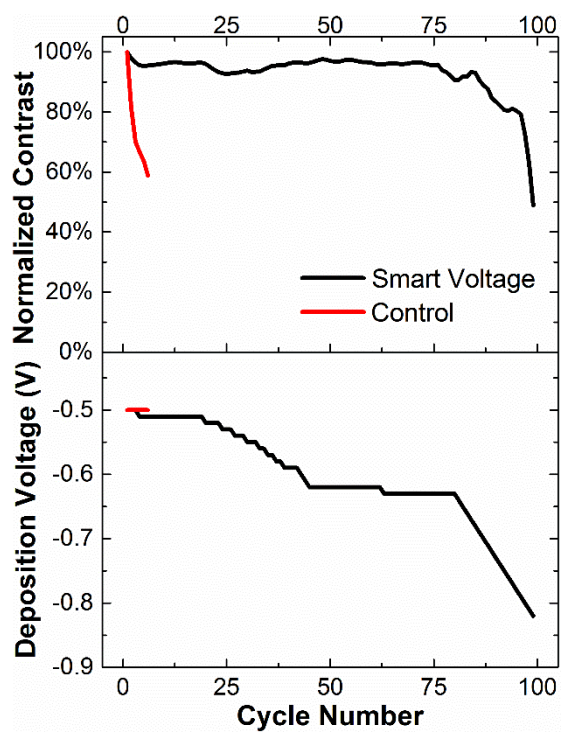


Figure 12: Normalized contrast ratio (top panel) of Zn dynamic windows with (black lines) and without (red lines) an optoelectronically-controlled algorithm and the voltage profiles used for deposition (bottom panel) during cycling. The time for deposition was held constant at 60 s. The stripping profile was also held constant at +0.8 V for 120 s.

Indeed, a control experiment cycling a Zn dynamic window with a constant voltage profile degrades to the 60% normalized cutoff after only six cycles (Figure 12, red lines). In contrast, when a Zn dynamic window is cycled using an algorithm that progressively increases the magnitude of the deposition potential, the normalized contrast ratio of the device does not decrease below the 60% threshold until 99 cycles (Figure 12, black lines). With the greater driving force of the more negative deposition voltages, the ZnO and Zn(OH)₂ electrodeposits are more readily converted into metallic Zn. As opposed to ZnO and Zn(OH)₂, which can only be dissolved chemically, metallic Zn electrodeposits can undergo rapid electrochemical stripping. For this reason, the more negative voltage deposition profile induced by the optoelectronic cycler increases stripping kinetics, thus improving device cycleability.

Bi-Prussian Blue Windows

Lastly, we also tested the optoelectronic cycler on windows utilizing Bi-Prussian blue chemistry (Figures 13 and S7). These windows combine a Bi electrolyte that facilitates Bi electrodeposition on the working electrolyte and a Prussian blue counter electrode that simultaneously darkens upon window tinting.¹⁵

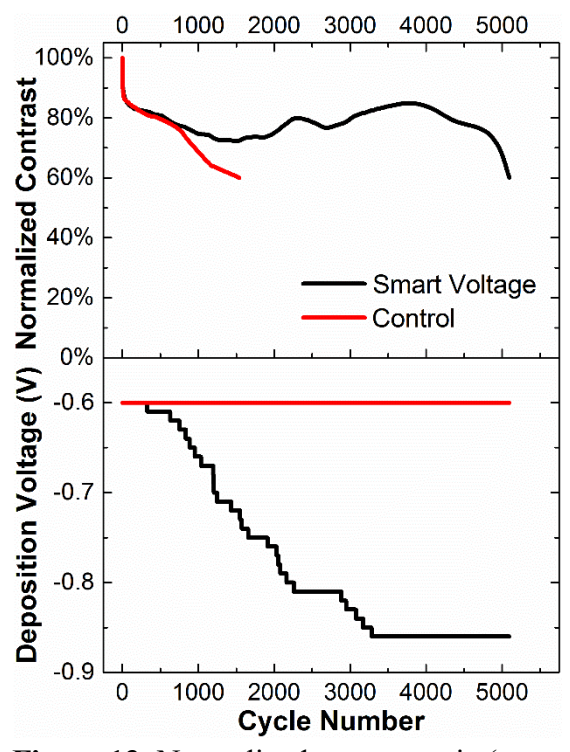


Figure 13: Normalized contrast ratio (top panel) of Bi-Prussian blue dynamic windows with (black lines) and without (red lines) an optoelectronically-controlled algorithm and the voltage profiles used for deposition (bottom panel) during cycling. The time for deposition was held constant at 20 s. The stripping profile was also held constant at +1.4 V for 45 s.

A Bi-Prussian blue dynamic window cycled with a constant voltage profile lasts 1,540 cycles before its normalized contrast ratio reaches the 60% cutoff value (Figure 13, red lines). By comparison, when an optoelectronically-controlled algorithm is used, the window cycles 5,094 times, which is more than a threefold improvement in cycle life (Figure 13, black lines). Previously, Bi-Prussian blue dynamic windows have been shown to have fast clearing times of only a few seconds. The algorithm here employs a clearing time of 45 s, which is much more

than is needed, at least during initial cycling. The algorithm instead progressively increases the magnitude of the deposition voltage, a strategy that is particularly effective given the wide electrochemical window for metal deposition with the Bi-Prussian blue chemistry (vMaxDark = -2.0 V). Given the results already described for the Bi-Cu windows with multiple algorithm variations, it is likely that adjustments in the Bi-Prussian blue switching algorithm would further increase device cycle life. Nonetheless, the 5,094 cycles demonstrated in this study represent one of the most durable 25 cm² dynamic windows based on reversible metal electrodeposition to be reported.

Applicability to Practical Dynamic Windows

The optoelectronic cycler designed here could be used to optimize voltage profiles for window chemistries, and those voltage profiles could subsequently be programmed into controllers for practical dynamic window products. Whereas our optoelectronic cycler is Windows-based and interfaces with modules via Python over USB, a dynamic window controller would likely take the form of a microcontroller system that is more compact and power efficient. The microcontroller would manage power electronics (such as switching regulators) for variable voltage application and track cycle counts to apply the predetermined voltage profile to the window. Optionally, to ensure stability if the dynamic window does not perform as expected to a voltage profile, the controller system could implement a light sensor to monitor performance and adjust the existing algorithm, similar to the optoelectronic cycler.

The concepts of the optoelectronic cycler developed in this work are fundamentally compatible with windows of any size. However, with sufficiently large windows, a few elements of the cycler would require modification. For example, different programmable power supplies that support larger currents would be needed. Furthermore, the two-inch linear actuator used in the

cycler for light sensor recalibration would have to be replaced with a longer actuator that can tolerate a heavier load.

Lastly, with dynamic windows substantially larger than the 25 cm² devices tested in this work, it is often important to quantify tinting uniformity. For RME windows, the voltage applied throughout the switching profile must be of a value such that metal electrodeposition is controlled by diffusion across the entire area of the electrode. As has been shown previously, this situation allows for uniform switching because metal electrodeposition occurs at an equal rate across the window. ¹⁹ An array of LEDs and light sensors positioned at different points across the dynamic window surface could be used to assess tinting uniformity. This information could then be utilized to adjust the voltage profile of the window during cycling to maintain uniform switching.

Conclusions

In conclusion, we developed an optoelectronic cycler for switching dynamic windows that allows for the development of complex voltage profile algorithms with real-time feedback from optical measurements. Because the individual components of the cycler are simple, a single-channel optoelectronic cycler costs less than \$1,000. We demonstrate how such cyclers can be applied to dynamic windows based on reversible metal deposition. In particular, the optoelectronic cycler is able to significantly increase the cycle lives of three different dynamic window chemistries. For all of these reasons, optoelectronic cyclers should aid dynamic window researchers in improving device durability in the laboratory setting.

Acknowledgments

This material is based upon work supported by the National Science Foundation Award under Grant No. ECCS2127308.

References

- 1. E. S. Lee, M. Yazdanian and S. E. Selkowitz, *Lawrence Berkeley National Laboratory*, LBNL (2004).
- 2. Energy Benefits of View Dynamic Glass in Workplaces, View Glass, Inc. https://view.com/sites/default/files/documents/workplace-white-paper.pdf Accessed 5/3/2022.
- 3. R. J. Mortimer, A. L. Dyer and J. R. Reynolds, *Displays*, **27**, 2 (2006).
- 4. C. G. Granqvist, M. A. Arvizu, İ. Bayrak Pehlivan, H. Y. Qu, R. T. Wen and G. A. Niklasson, *Electrochim. Acta*, **259**, 1170 (2018).
- 5. D. Coates, J. Mater. Chem., 5, 2063 (1995).
- 6. S. Araki, K. Nakamura, K. Kobayashi, A. Tsuboi and N. Kobayashi, *Adv. Mater.*, **24**, OP122 (2012).
- 7. A. Tsuboi, K. Nakamura and N. Kobayashi, *Adv. Mater.*, **25**, 3197 (2013).
- 8. X. Guo, J. Chen, A. L.-S. Eh, W. C. Poh, F. Jiang, F. Jiang, J. Chen and P. S. Lee, *ACS Appl. Mater. Interfaces* (2022).
- 9. C.-G. Granqvist, Nat. Mater., 5, 89 (2006).
- 10. American Society for Testing and Materials, ASTM E2141-14, Standard Test Method for Accelerated Aging of Electrochromic Devices in Sealed Insulating Glass Units.
- 11. H. S. Bergh, J. Bass, J. Ziebarth, N. Timmerman, Z. Hogan, K. Yaccato and H. Turner. U.S. Patent No: US8717658B2 (2012).
- 12. C. Larson and J. P. G. Farr, Transactions of the IMF, 88, 237 (2010).
- 13. C. L. DeFoor, J. F. Jeanetta and C. J. Barile, ACS Appl. Electron. Mater., 2, 290 (2020).
- 14. C. J. Barile, *J. Appl. Electrochem.*, **48**, 443 (2018).
- 15. S. M. Islam and C. J. Barile, ACS Appl. Mater. Interfaces, 11, 40043 (2019).
- 16. T. S. Hernandez, C. J. Barile, M. T. Strand, T. E. Dayrit, D. J. Slotcavage and M. D. McGehee, *ACS Energy Lett.*, **3**, 104 (2018).
- 17. S. M. Islam and C. J. Barile, Adv. Energy Mater., 11, 2100417 (2021).
- 18. C. J. Barile, D. J. Slotcavage, J. Hou, M. T. Strand, T. S. Hernandez and M. D. McGehee, *Joule*, 1, 133 (2017).
- 19. M. T. Strand, C. J. Barile, T. S. Hernandez, T. E. Dayrit, L. Bertoluzzi, D. J. Slotcavage and M. D. McGehee, *ACS Energy Lett.*, **3**, 2823 (2018).
- 20. S. M. Islam, A. A. Palma, R. P. Gautam and C. J. Barile, *ACS Appl. Mater. Interfaces*, **12**, 44874 (2020).
- 21. S. M. Islam, C. N. Fini and C. J. Barile, J. Electrochem. Soc., 166, D333 (2019).
- 22. T. S. Hernandez, M. Alshurafa, M. T. Strand, A. L. Yeang, M. G. Danner, C. J. Barile and M. D. McGehee, *Joule*, 4, 1501 (2020).
- 23. S. M. Islam, T. S. Hernandez, M. D. McGehee and C. J. Barile, Nat. Energy, 4, 223 (2019).
- 24. D. C. Madu, S. M. Islam, H. Pan and C. J. Barile, *J. Mater. Chem. C*, **9**, 6297 (2021).